SLAC–PUB–6678
October 1994
(T/E)

PRECISION STANDARD MODEL TESTS WITH POLARIZED e^+e^- BEAMS*

Michael J. Fero

Massachusetts Institute of Technology, Cambridge, Massachusetts 0213
and
Stanford Linear Accelerator Center. Stanford University, Stanford, CA 94309

REPRESENTING THE SLD COLLABORATION◇

ABSTRACT

The advent of polarized electron beams at the Stanford Linear Collider (SLC) makes possible the new precision electroweak tests now being performed by the SLC Large Detector (SLD) experiment. One such new technique, the left-right asymmetry measurement, allows remarkably direct measurement of the effective weak mixing angle, $\sin^2\theta_W^{\rm eff} = 0.2292 \pm 0.0009({\rm stat}) \pm 0.0004({\rm syst})$. When considered within the Minimal Standard Model (MSM) framework, this result predicts the top mass to be $m_t = 240^{+30+18}_{-45-20}$ GeV where the first errors are experimental and the second reflect a range of possible Higgs mass values from 60 to 1000 GeV.

Invited talk presented at the XIV International Conference on Physics in Collision
Tallahassee, Florida, June 15–17, 1994

*Work supported in part by Department of Energy contract DE–AC03–76SF00515 (SLAC), the National Science . Foundation, the Istituto Nazionale di Fisica Nucleare of Italy, the Japan–U.S. Cooperative Research Project on High Energy Physics, and the Science and Engineering Research Council of the United Kingdom.
◇Collaboration members and their institutes are listed following the references.

1 Introduction

There has been a dedicated effort for the last several years to extract precision information about the validity of the Standard Model. With the vast amount of precision electroweak (EW) data now emerging from the Large Electron Positron Collider (LEP) [1, 2] and the recent progress in determining the top mass at the Collider Detector at Fermilab (CDF) and D0 [3, 4, 5], experimenters will soon tightly overconstrain the standard model, and thus test it in a rigorous way. What can be added to the discussion from the results now coming out of the SLD experiment at the polarized SLC? In principle the SLD and the LEP experiments are measuring very similar physical quantities. However, the polarized beam at the SLC is a unique tool, enabling the experimenter to make remarkably precise measurements of standard model quantities with systematic errors that are small and differ radically from the types of systematic errors encountered by the LEP experiments. In this paper I briefly describe some of the common electroweak standard model tests done at the Z-pole and then show, in some detail, how a new test at the Polarized SLC is performed and some recent results.

2 Precision Tests of the Standard Model

2.1 Electroweak Parameters

The dynamics of the electroweak sector of the Standard Model are determined to lowest order by three parameters: the SU(2) coupling constant, g, the U(1) coupling constant, g', and the vacuum expectation value of the Higgs field, $\langle\phi\rangle$. The values of these parameters can be extracted from a number of related experimental quantities, a few of which are listed in Table 1. With the high-precision mass measurements of the Z from LEP, the experimental quantities determining the Standard Model are taken to be: the electromagnetic fine structure constant, α, the fermi coupling constant, G_F, and the mass of the Z boson, M_Z.

Additional measurements of electroweak observables (such as the Z width, Γ_Z, the W mass, M_W, and the effective weak mixing angle $\sin^2\theta_W^{\rm eff}$) should then overconstrain the model. However, the expressions in Table 1 relating M_Z, M_W, Γ_Z and $\sin^2\theta_W^{\rm eff}$, to g, g', and $\langle\phi\rangle$ are valid only to lowest order. Virtual electroweak corrections that depend on the top quark mass and Higgs boson mass must be included. Only within the uncertainties due to the lack of knowledge of the top and Higgs masses do the measurements of additional electroweak quantities serve to overconstrain the model, and thus test it. That test may well be at hand, however, with precise top mass measurements expected soon from the Tevatron

Table 1. Quantities that determine Standard Model parameters. The first three define the Minimal Standard Model while the additional measurements can serve to overconstrain it.

Quantity	Electroweak Parameter	Current Value	Precision (ppm)	Cite
α	$(1/4\pi)\ [\mathrm{g}^2\mathrm{g}'^2/(\mathrm{g}^2+\mathrm{g}'^2)]$	$1/137.0359895(61)$	0.045	[6]
G_F	$(\sqrt{2}/2)\ (1/\langle\phi\rangle^2)$	$1.16639(2)\times10^{-5}$ GeV	17	[6]
M_Z	$\frac{1}{2}\ \langle\phi\rangle\ \sqrt{g^2+g'^2}$	91.1888 ± 0.0044 GeV	48	[2]
Γ_Z	$\left[\langle\phi\rangle\ (g^2+g'^2)^{3/2}\ /\ 384\pi\right] \times \left\{1+[(1-4Q_f g'^2/(g^2+g'^2)]^2\right\}$	2.4974 ± 0.0038 GeV	1522	[2]
M_W	$\langle\phi\rangle g/2$	80.23 ± 0.18 GeV	2244	[7]
$\sin^2\theta_W^{\mathrm{eff}}$	$g'^2/(g^2+g'^2)$	0.2322 ± 0.0004	1723	[2]

experiments. Those measurements, together with the body of Electroweak measurements from the Z-pole asymmetries, the Z-width and W-mass measurements, the neutrino-nucleon scattering experiments, and the atomic-parity violation experiments will combine to put interesting limits on the validity of the Standard Model.

This talk focuses on a precision measurement of the weak mixing angle ($\sin^2\theta_W^{\mathrm{eff}}$), where polarized beams at SLC can make a particularly significant contribution.

2.2 The $\sin^2\theta_W^{\mathrm{eff}}$ Measurements

The mixing angle $\sin^2\theta_W^{\mathrm{eff}}$ is defined here in terms of the vector (v_f) and axial vector (a_f) couplings of the Z to fermion pairs,

$$\begin{aligned} a_f &= T_f^3 \\ v_f &= T_f^3 - 2Q_f\ \sin^2\theta_W^{\mathrm{eff}}\ , \end{aligned}$$

where T_f^3 is the third component of weak isospin for fermion f, and Q_f is the charge of the fermion. The eff superscript stands for effective and refers to the fact that the weak mixing angle can be defined in a number of ways—in this case, through fermion couplings at the Z. The weak mixing angle $\sin^2\theta_W^{\mathrm{eff}}$ can be measured through a variety of techniques at the Z-pole, but the important measurements can be classified as follows: forward-backward cross section asymmetries of the Z into final state leptons, A_{FB}^l, forward-backward cross section asymmetries of the Z into final state quarks, A_{FB}^q, measurement of the tau polarization, $\mathcal{P}_\tau$, and measurement of the left-right cross section asymmetry for the production of Z

Table 2. Qualitative comparison of measurements from different Z-pole asymmetry experiments.

Property	A_{LR}	A^l_{FB}	A^b_{FB}	$\mathcal{P}_\tau$
Asymmetry	$0.16 \times \mathcal{P}_e$	0.02	0.11	0.16
Sensitivity to $\sin^2\theta_W^{\rm eff}$	$7.9 \times \mathcal{P}_e$	1.5	5.6	7.9
Fraction of Z decays	0.96	0.12	0.19	0.04
Efficiency $\times$ acceptance	0.90	0.8	0.10	0.03
Relative Z sample	1	150	60	200
Beam Polarization	Yes	No	No	No
Efficiency $\times$ acceptance	No	Yes	Yes	Yes
Backgrounds	No	No	Yes	Yes
B-Mixing	No	No	Yes	No
EW interference correction	2%	100%	5%	2%

particles by polarized electrons on unpolarized positrons, A_{LR}. The first three categories of measurement have been well described in the talk by A. Olchevski [1], so the measurement types are summarized and a discussion of A_{LR} follows.

The lepton forward-backward asymmetries, A^l_{FB} at the Z-pole are defined as

$$A^l_{FB} \;=\; \frac{\sigma^l_F - \sigma^l_B}{\sigma^l_F + \sigma^l_B} \;=\; \frac{3}{4}\mathcal{A}_e\mathcal{A}_l \; . \tag{1}$$

where the asymmetry term for a particular fermion species is given in general by

$$\mathcal{A}_f = \frac{2v_f a_f}{v_f^2 + a_f^2} \; . \tag{2}$$

Similarly, for the quark forward-backward asymmetries A^q_{FB} at the Z-pole, the simple definition is

$$A^q_{FB} \;=\; \frac{\sigma^q_F - \sigma^q_B}{\sigma^q_F + \sigma^q_B} \;=\; \frac{3}{4}\mathcal{A}_e\mathcal{A}_q \; , \tag{3}$$

with the somewhat more arduous task of tagging a final state heavy quark ($q = b, c$). It is important to note that for the all of the forward-backward asymmetries, the sensitivity to $\sin^2\theta_W^{\rm eff}$ comes largely from the lepton factors $\mathcal{A}_e$. The sensitivity of the asymmetry factors to $\sin^2\theta_W^{\rm eff}$ is given roughly by $\partial\mathcal{A}_e/\partial s \sim -7.9$, $\partial\mathcal{A}_b/\partial s \sim -0.6$, and $\partial\mathcal{A}_c/\partial s \sim -3.4$, with s=$\sin^2\theta_W^{\rm eff}$.

Obviously, the lepton couplings are most sensitive to $\sin^2\theta_W^{\rm eff}$, the up-type quarks have modest sensitivity, while the down-type quarks have very little sensitivity to $\sin^2\theta_W^{\rm eff}$. A summary of the experimental sensitivities, as well as some other qualitative comparisons, is given in Table 2.

The tau polarization measurement is another interesting way to get at the leptonic couplings. The polarization of the tau as a function of production angle is determined by the initial and final state couplings of the Z, and is given by

$$\mathcal{P}_\tau = \frac{\sigma_R - \sigma_L}{\sigma_R + \sigma_L} = -\frac{\mathcal{A}_\tau(1+\cos^2\theta) + 2\mathcal{A}_e\cos\theta}{(1+\cos^2\theta) + 2\mathcal{A}_l\mathcal{A}_e\cos\theta} , \tag{4}$$

so that it is possible to extract both the $\mathcal{A}_e$ and $\mathcal{A}_\tau$ asymmetries in a single measurement.

Finally, there is the left-right asymmetry. Almost embarrassingly simple, it measures the electron coupling asymmetry directly by just counting the number of Z bosons produced with left- versus right-handed electron beam, moderated by the degree of polarization of the electron beam $\mathcal{P}_e$,

$$A_{LR} = \frac{\sigma_L - \sigma_R}{\sigma_L + \sigma_R} = \mathcal{P}_e \cdot \mathcal{A}_e . \tag{5}$$

Obviously, a good measure of the electron beam polarization is important, since it scales the result—a precise, yet inaccurate, measurement of the polarization would be unfortunate!

3 Precision Tests with Polarized Beams at the SLC

The SLC is the worlds first, and only, single pass e^+e^- colliding beam facility (linear collider). A diagram of the SLC is shown in Figure 1. The machine was designed to copiously produce Z bosons in a low background environment. Because of the experimental nature of the machine, achieving design luminosity has been a substantial challenge. The SLC machine was also designed to accommodate polarized electron beams, thus providing a unique tool for probing the electroweak interaction [8]. The SLC was completed in 1987, and the first Z bosons produced in e^+e^- collisions were observed in the same year by the MARKII detector. The SLC underwent an extensive commissioning period that saw the retirement of the MARKII detector in 1990. The new SLD detector replaced the MARKII in 1991, and began its run with steadily increasing luminosity and greater SLC reliability. In 1992, the SLC began producing Z bosons with a longitudinally polarized electron beam, and by the end of the run the SLD experiment had recorded over 10,000 Z events produced with $> 20\%$ polarized electron beam. For the 1993 run, the advent of strained lattice cathodes[**?**] resulted in beam polarization in excess of 60% measured at the SLC interaction point, while increases in machine luminosity allowed the SLD to record over 50,000 Z events produced with polarized beam. Further development of the strained lattice cathodes has resulted in beam polarization of $\sim 80\%$ at the SLC interaction point. This is an important achievement. Since the statistical precision of the $\sin^2\theta_W^{\rm eff}$ measurement is sensitive to the square of the beam polarization, the factor-of-four increase in beam polarization experienced at SLC is equivalent to a factor of sixteen increase in machine luminosity!

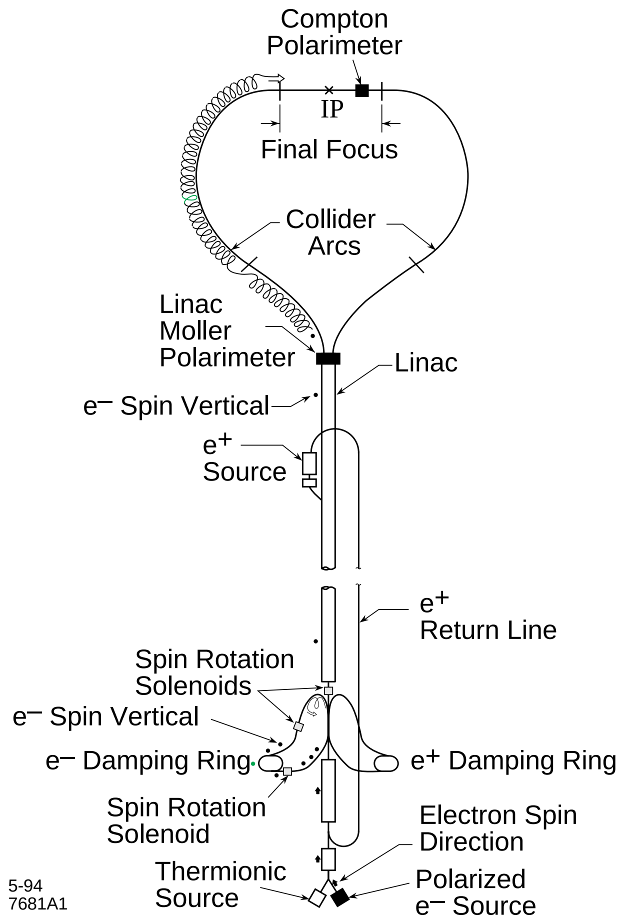

Figure 1: The layout of the SLC showing polarization related features.

3.1 Polarized Beams at the SLC

For the electroweak asymmetry measurements, it is necessary to know the degree of longitudinal electron beam polarization as seen by the positrons that produce Z bosons. In practice, a Compton-scattering based polarimeter is used *near* the interaction point (32 meters downstream of the SLC interaction point) to measure beam polarization, $\mathcal{P}_e^C$ [9]. Figure 2 shows a schematic view of the polarimeter. This polarimeter detects Compton-scattered electrons from the collision of the longitudinally polarized electron beam with a circularly polarized photon beam; the photon beam is produced from a pulsed Nd:YAG laser operating at 532 nm. After Compton scattering off of the photon beam, the electrons pass through a dipole spectrometer; a nine-channel Čerenkov detector then measures electrons in the range 17 to 30 GeV.

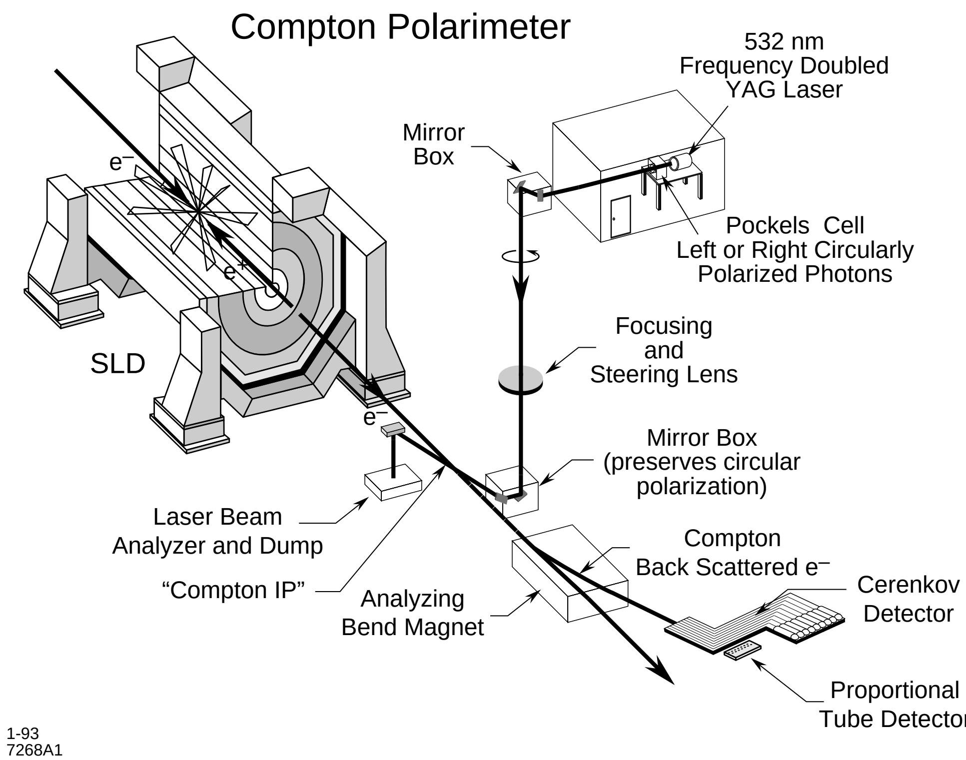

Figure 2: An overview of the Compton Polarimeter at the SLC.

3.1.1 Polarization Measurement

The counting rates in each Čerenkov channel are measured for parallel and antiparallel combinations of the photon and electron beam helicities. The asymmetry formed from these rates is given by

$$A(E) \;=\; \frac{R(\rightarrow\rightarrow) - R(\rightarrow\leftarrow)}{R(\rightarrow\rightarrow) + R(\rightarrow\leftarrow)} \;=\; \mathcal{P}_e^C \mathcal{P}_\gamma A_C(E) \;, \tag{6}$$

where $\mathcal{P}_\gamma$ is the circular polarization of the laser beam at the Compton interaction point, and $A_C(E)$ is the Compton asymmetry function. Measurements of $\mathcal{P}_\gamma$ are made before and after the Compton interaction point. By monitoring and correcting for small phase shifts in the laser transport line, SLD is able to achieve $\mathcal{P}_\gamma = (99 \pm 1)\%$. Figure 3 shows the dependence of the unpolarized Compton cross section and Compton asymmetry $A_C(E)$ on transverse distance from the undeflected beamline. Also shown are the nominal acceptances of the nine Čerenkov channels. The photon energy of the laser beam is $E_\gamma = 2.33$ eV, so that with an electron beam energy of 45.68 GeV, an electron that is fully back-scattered in the cms frame will have an energy of 17.4 GeV in the lab frame. This places the kinematic endpoint of the Compton spectrum 17 cm from the undeflected beamline. The Compton asymmetry crosses

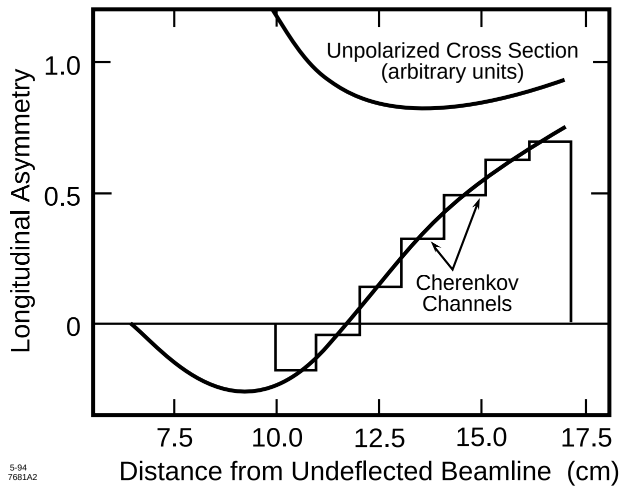

Figure 3: The Compton asymmetry as a function of distance from the undeflected beam line. Channel acceptances for the Čerenkov detector are also shown.

through zero at an electron energy of 25.2 GeV, corresponding to a transverse position of 11.7 cm from the undeflected beamline. Figure 3 shows that both of these points lie well within the acceptance of the Čerenkov detector. The detector can thus be fully calibrated with information provided by the scattering spectrum itself, while *a priori* knowledge of the beam and detector position and of the bend strength of the analyzing magnets can be reserved for a consistency check [10]. Detector resolution effects modify $A_C(E)$. This effect is about 1% for the Čerenkov channel at the Compton edge. Detector position scans are used to locate the Compton edge. The position of the zero-asymmetry point is then used to fit for the spectrometer dipole bend strength. Once the detector energy scale is calibrated, each Čerenkov channel provides an independent measurement of $\mathcal{P}_e^C$. The beam polarization is determined using channels 6 and 7, channels 1–5 are used as a cross-check, and deviations of the measured asymmetry spectrum from the modeled one are reflected in the interchannel consistency systematic error. Figure 4 shows the good agreement achieved between the measured and simulated Compton asymmetry spectrum.

Polarimeter data are acquired continually during the operation of the SLC. The measured beam polarization is typically 61–64%. The absolute statistical precision attained in a 3-minute interval is typically $\delta\mathcal{P}_e^C = 1.0\%$. Averaged over the 1993 run, the mean beam polarization is found to be $\mathcal{P}_e^C = (61.9 \pm 0.8)\%$. The systematic uncertainties that affect the polarization measurement are summarized in Table 3.

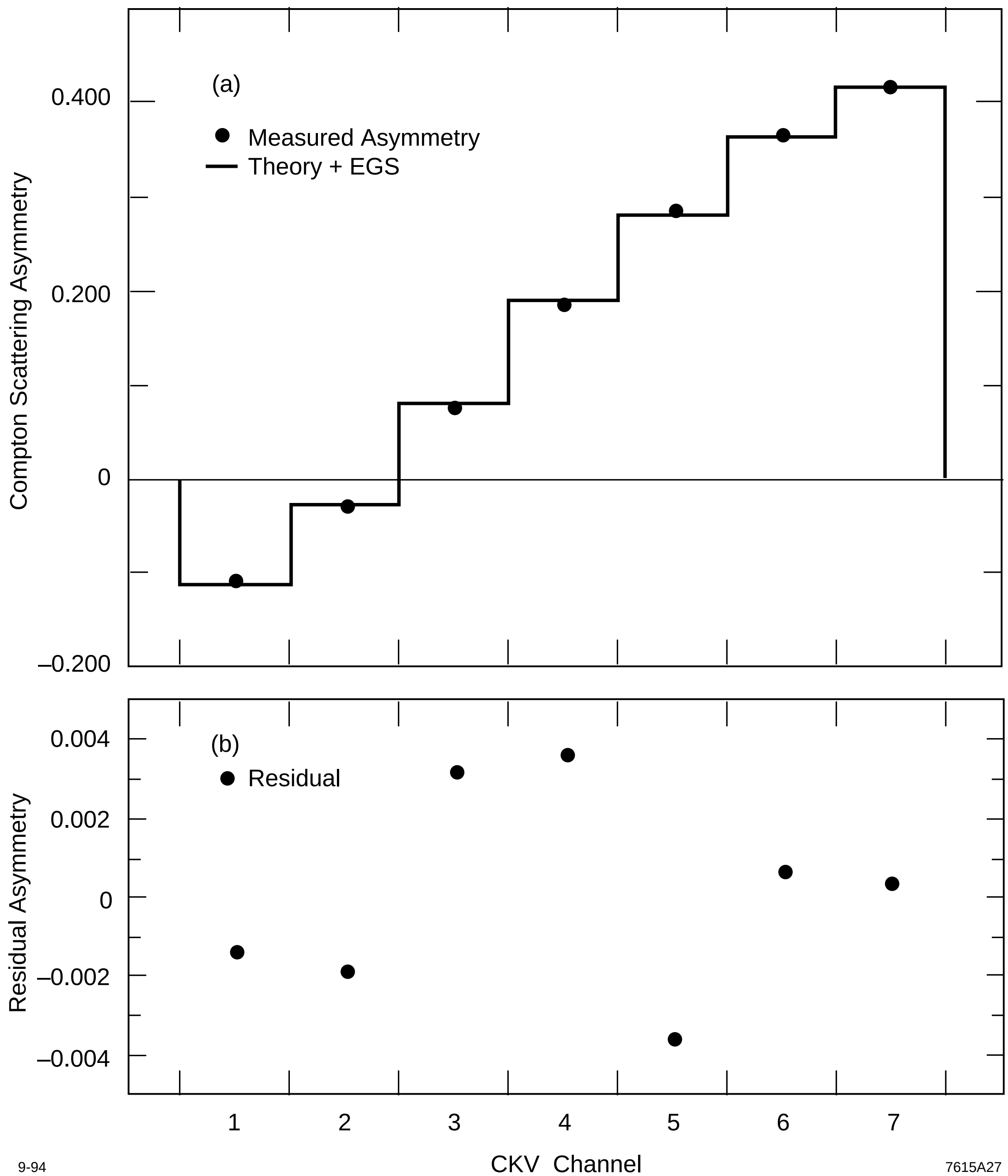

Figure 4: Comparison of the measured Compton asymmetry and the theoretical asymmetry, including the EGS detector response function. The residuals are shown in the inset

Table 3. Systematic uncertainties on the A_{LR} measurement.

Systematic Uncertainty	$\delta\mathcal{P}_e/\mathcal{P}_e$ (%)	$\delta A_{LR}/A_{LR}$ (%)
Laser polarization	1.0	
Detector calibration	0.4	
Detector linearity	0.6	
Interchannel consistency	0.5	
Electronic noise	0.2	
Total polarization uncertainty	1.3	1.3
Chromaticity correction (ξ)		1.1
Total(y) small corrections		0.1
Total systematic uncertainty		1.7

3.1.2 The chromatic effect

The Compton polarimeter measures the average beam polarization over the entire electron bunch $\mathcal{P}_e^C$, 32 m from the SLC interaction point. This polarization can differ slightly from the polarization of the beam that annihilates to produce Z bosons P_e. Effects due to beam disruption of the electron bunch by the positron bunch, or spin rotation due to quadrupoles between the SLC interaction point and the Compton interaction point, have been shown to be negligible. However, a chromatic effect at the SLC interaction point is not. Because of the electron-energy dependent rate of spin precession in the SLC Arc, the off-nominal energy tails of the beam have a different net longitudinal polarization at the SLC interaction point than does the core of the beam. In the chromatic effect, off-energy electrons are not well focused at the SLC interaction point, and thus cannot contribute to luminosity. Therefore, the polarization of the beam that produces luminosity is different than the total beam polarization. This implies that the instantaneous polarization at the SLC interaction point will be a weighted average over number density, luminosity, and polarization as functions of energy:

$$\mathcal{P}_e = \frac{\int n(E)\ \mathcal{P}(E)\ \mathcal{L}(E)\ dE}{\int n(E)\ \mathcal{L}(E)\ dE} \ . \tag{7}$$

The Compton polarimeter, with its interaction point at a place of low-dispersion downstream of the SLC interaction point, measures the total beam polarization, which is the same as the SLC interaction-point polarization in the case where the luminosity is constant with energy,

$$\mathcal{P}_e^C = \frac{\int n(E)\ \mathcal{P}(E)\ dE}{\int n(E)\ dE} \ . \tag{8}$$

The SLD characterizes the difference between the SLC interaction point and Compton interaction point polarizations with a single parameter ξ, referred to as the *chromaticity correction*,

$$\mathcal{P}_e \;=\; (1+\xi)\;\mathcal{P}_e^C \;. \tag{9}$$

The size of the chromaticity effect can be estimated from a simple chromaticity model. The inputs to the model are shown in Figure 5. With the luminosity given by

$$\mathcal{L}(E) \;=\; \frac{N^+(E)\;N^-(E)}{4\pi\;\sigma_x(E)\;\sigma_y(E)} \;, \tag{10}$$

we see that calculation of the size of the effect requires some knowledge of the spot size dependence on energy. This is taken from a simple model of the chromatic effects in the SLC final focus [11]. The other required inputs are the intensity versus energy profile, $n(E)$ (found by measuring scattered radiation as a thin wire is scanned across the SLC electron beam at a high dispersion point), and the polarization $\mathcal{P}(E)$ versus energy profile (measured directly by varying the beam energy and monitoring polarization). For the Gaussian core of the beam $\Delta E/E = 0.2\%$, the model predicts a small effect $\xi < 0.002$. However, $n(E)$ has a low-energy tail extending to $\Delta E/E = 1\%$, with correspondingly low polarization and large beam size. With this effect, the size of the chromaticity correction is estimated to be $\xi = 0.019 \pm 0.005$.

A more rigorous bound on the size of the chromaticity effect can be made using a conservative, essentially model-independent estimate based on experimental observations. The chromaticity correction is rigorously limited by the relation

$$(1-\xi) \;\leq\; \left[\frac{\mathcal{P}_e^C(\Delta E/E=0)}{\mathcal{P}_e^C}\right]_{\max} \left[\frac{\mathcal{P}_e}{\mathcal{P}_e^C(\Delta E/E=0)}\right]_{\max} \;, \tag{11}$$

where SLD determines the upper limit on ξ by finding the upper limit on the two polarization ratios defined in this equation. Comparison of the polarization of a monochromatic beam, $\mathcal{P}_e^C(\Delta E/E = 0)$, versus a normal energy spread beam, $\mathcal{P}_e^C$, comes from direct measurement. In special tests, the core width of the electron beam energy distribution was reduced to less than 0.1% and the low-energy tail was removed by overcompressing the beam in the damping ring. In this configuration, the Compton polarimeter measures the beam polarization with spin diffusion made negligible, since the energy spread of the beam has been made negligible. When compared to the measured polarization during normal beam running, the first of the two ratios is then

$$\frac{\mathcal{P}_e^C(\Delta E/E=0)}{\mathcal{P}_e^C} \;=\; \frac{(65.7\pm 0.6)}{(63.15\pm 0.01)} \;=\; 1.0438 \pm 0.0005 < 1.0628 \;(95\%\ \text{C.L.}) \quad . \tag{12}$$

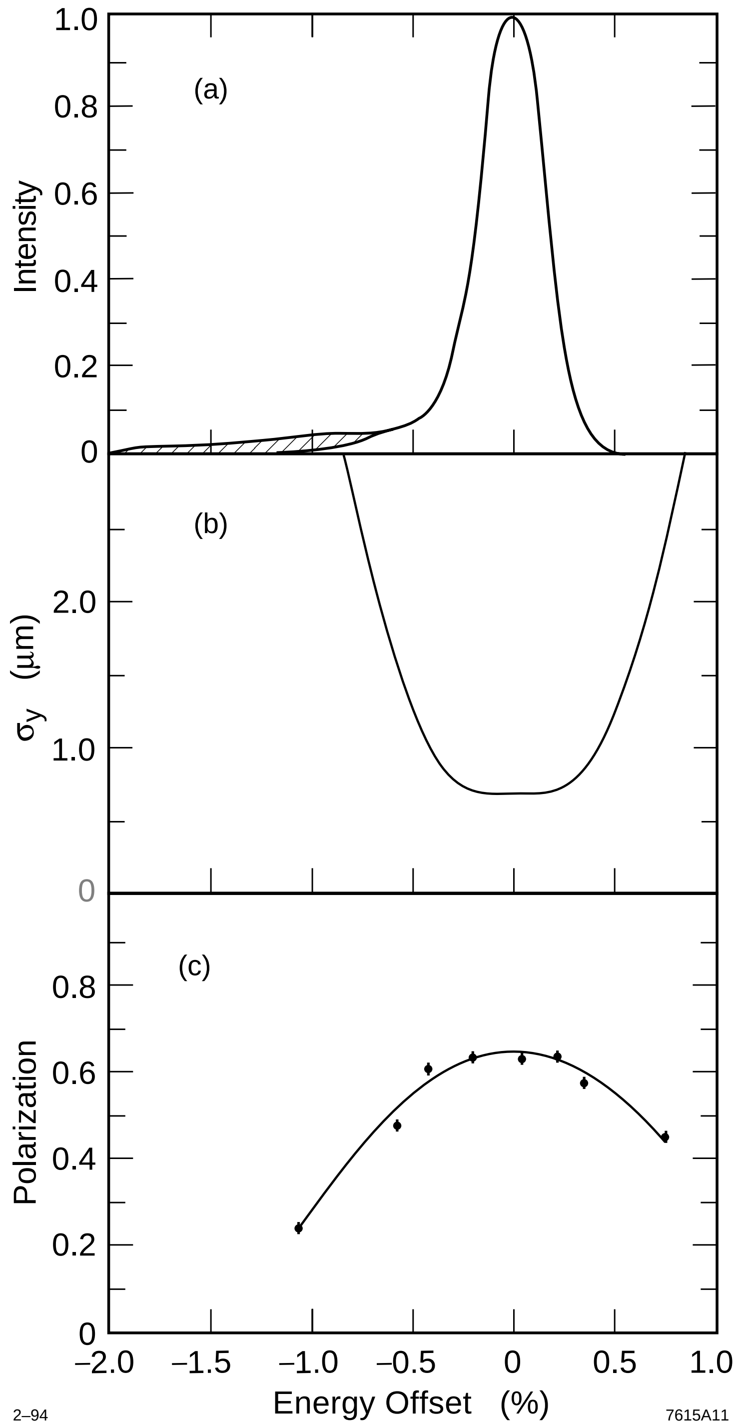

Figure 5: Three inputs to the luminosity weighted polarization are (a) the intensity versus energy, $n(E)$, (b) the spot size as a function of energy, $\sigma(E)$, and (c) the polarization versus energy, $\mathcal{P}(E)$.

A bound on the second ratio is found by noting that $\mathcal{P}_e$ must be less than $\mathcal{P}_e(\Delta E/E = 0)$, and that the ratio is at most unity. The SLD makes a conservative estimate, assuming that the energy tail of the beam does not contribute to the luminosity weighted polarization and that all of the polarization comes from the core of the beam. The upper bound on this ratio is determined by a TURTLE transport simulation of the arc and final focus region, with the conservative (that is, tending to maximize the ratio) beam parameters listed in Table 4.

Table 4. Beam parameters used in chromatic effect estimate.

Parameter	Assumed Limit
$\theta_y^{\rm rms}$	$< 200\ \mu$rad
$\theta_x^{\rm rms}$	$< 300\ \mu$rad
ϵ_y	$> 650\ \mu$m-rad
ϵ_x	$> 100\ \mu$m-rad
σ_E	$> 0.15\%$
$\mathcal{P}_e/\mathcal{P}_e(\Delta E/E = 0)$	< 0.986

This gives the upper limit

$$\frac{\mathcal{P}_e}{\mathcal{P}_e^C\ (\Delta E/E = 0)} \ < \ 0.986 \text{ (95\% C.L.)} \tag{13}$$

for the ratio of normal polarization to that which would be seen with a monochromatic beam. The limit on the chromaticity correction is thus $0 \leq \xi \leq 0.048$. The central value is taken as the correction, and the width as the error, $\xi = 0.024 \pm 0.016$.

3.2 The Left-Right Asymmetry A_{LR}.

3.2.1 Event selection and analysis

The e^+e^- collisions are measured by the SLD detector with a trigger that relies on a combination of calorimeter and tracking information. In order to maximize the number of events available for the A_{LR} measurement in the sometimes harsh background environment of the SLC the event selection is entirely based on the liquid argon calorimeter [14]. The combined efficiency of the SLD trigger and selection criteria is (93±1)% for hadronic Z decays. Less than 1% of the sample consists of tau pairs. Muon pair events deposit only small energy in the calorimeter; they are not included in the sample. The residual background in the sample is due primarily to beam-related backgrounds and e^+e^- final state events. From the data, SLD estimates the background fraction due to these sources to be $(0.23 \pm 0.10)\%$. The background fraction due to cosmic rays and two-photon processes is (0.02±0.01)%.

Using the detector, the number (N_L, N_R) of hadronic and $\tau^+\tau^-$ decays of the Z boson for each of the two longitudinal polarization states (L,R) of the electron beam is counted. The electron beam polarization is measured precisely with the polarimeter. The measurement does not require knowledge of the absolute luminosity, detector acceptance, or detector efficiency.

Applying the selection criteria, SLD counts 27,225 (N_L) events produced with the left-polarized electron beam and 22,167 (N_R) were produced with the right-polarized beam. The measured left-right cross section asymmetry for Z production is

$$A_m \equiv (N_L - N_R) \Big/ (N_L + N_R) = 0.1024 \pm 0.0045 . \tag{14}$$

The measured asymmetry A_m does not vary significantly as more restrictive criteria (calorimetric and tracking based) are applied to the sample, and A_m is uniform when binned by the azimuth and polar angle of the thrust axis.

The measured asymmetry A_m is related to A_{LR} by the following expression, which incorporates a number of small correction terms in lowest-order approximation,

$$A_{LR} = \frac{A_m}{\langle \mathcal{P}_e \rangle} + \frac{1}{\langle \mathcal{P}_e \rangle}\left[f_b(A_m - A_b) - A_{\mathcal{L}} + A_m^2 A_{\mathcal{P}} - E_{cm}\,\frac{\sigma'(E_{cm})}{\sigma(E_{cm})}\,A_E - A_\varepsilon + \langle \mathcal{P}_e \rangle \mathcal{P}_{e^+} \right] , \tag{15}$$

where $\langle \mathcal{P}_e \rangle$ is the mean luminosity-weighted polarization for the 1993 run; f_b is the background fraction; $\sigma(E)$ is the unpolarized Z cross section at energy E; $\sigma'(E)$ is the derivative of the cross section with respect to E; $\mathcal{P}_{e^+}$ is any longitudinal positron polarization assumed to have constant helicity [12], and A_b, $A_{\mathcal{L}}$, $A_{\mathcal{P}}$, A_E, and A_ε are the left-right asymmetries of the residual background, the integrated luminosity, the beam polarization, the center-of-mass energy, and the product of detector acceptance and efficiency, respectively.

The luminosity-weighted average polarization $\langle \mathcal{P}_e \rangle$ is estimated from measurements of $\mathcal{P}_e$ made when Z events were recorded,

$$\langle \mathcal{P}_e \rangle = (1 + \xi)\,\frac{1}{N_Z} \sum_{i=1}^{N_Z} \mathcal{P}_i = (0.630 \pm 0.011) , \tag{16}$$

where N_Z is the total number of Z events and $\mathcal{P}_i$ is the polarization measurement associated in time with the ith event. The error on $\langle \mathcal{P}_e \rangle$ is dominated by the systematic uncertainties on the polarization measurement and the chromaticity correction, ξ.

Table 5. Small corrections to A_{LR}: a comprehensive list of possible sources of error on the A_{LR} measurement. None are significant.

Correction	Parameter	Value (10^{-4})	$\Delta A_{LR}/A_{LR}$ (%)
Background fraction	f_b	23 ± 10	0.17 ± 0.07
Background asymmetry	A_b	310 ± 100	
Efficiency asymmetry	A_ϵ	≈ 0	≈ 0
Luminosity asymmetry	$A_\mathcal{L}$	0.38 ± 0.50	-0.037 ± 0.049
Polarization asymmetry	$A_\mathcal{P}$	-33 ± 1	-0.034 ± 0.001
Energy asymmetry	A_E	0.0044	0.00085 ± 0.00002
Positron polarization	$\mathcal{P}_{e^+}$	< 0.15	< 0.0009
Total correction			0.10 ± 0.08

The corrections defined in square brackets in Equation (15) are very small; for completeness, they are shown in Table 5.

Of these corrections, the most significant one is that due to background contamination. The correction for this is moderated by a non-zero left-right background asymmetry ($A_b = 0.031 \pm 0.010$) arising from e^+e^- final states that remain in the sample. Backgrounds give a net fractional correction to A_{LR} of $(+0.17 \pm 0.07)\%$.

The corrections in Equation (15) give a net correction to A_{LR} of only $(+0.10 \pm 0.08)\%$ of the uncorrected value. The contributions to the systematic error are summarized in Table 3.

3.2.2 Results

Using Equation (15), SLD finds the left-right asymmetry to be

$$A_{LR}\,(91.26 \text{ GeV}) \;=\; 0.1628 \pm 0.0071\,(\text{stat}) \pm 0.0028\,(\text{syst}) \;. \tag{17}$$

This result is corrected to account for photon exchange and for electroweak interference that arises from the deviation of the effective e^+e^- center-of-mass energy from the Z-pole energy (including the effect of initial-state radiation). The result for pole asymmetry A^0_{LR} and the effective weak mixing angle is

$$\begin{aligned} A^0_{LR} \;&=\; 0.1656 \pm 0.0071\,(\text{stat}) \pm 0.0028\,(\text{syst}) \;, \\ \sin^2\theta_W^{\text{eff}} \;&=\; 0.2292 \pm 0.0009\,(\text{stat}) \pm 0.0004\,(\text{syst}) \;. \end{aligned} \tag{18}$$

The experiment also cites the result of this measurement, combined with their previous measurement [14] with 10,000 Z bosons at 20% polarization—statistically weak by comparison, for a value of $\sin^2\theta_W^{\rm eff} = 0.2294 \pm 0.0010$, corresponding to the pole asymmetry, $A_{LR}^0 = 0.1637 \pm 0.0075$ [15].

4 Conclusions

We note that with this measurement SLD has made the most precise single determination of $\sin^2\theta_W^{\rm eff}$ to date. When considered within the MSM framework, this result predicts the top mass to be $m_t = 240^{+30+18}_{-45-20}$ GeV, where the first errors are experimental and the second reflect a range of possible Higgs mass values from 60 to 1000 GeV. This $\sin^2\theta_W^{\rm eff}$ determination is smaller by 2.5 standard deviations than a recent LEP average value 0.2322 ± 0.0004 extracted from measurements of the forward-backward asymmetries of leptonic, hadronic, b-quark, and c-quark final states and those of the polarization of tau lepton final states (assuming universality of the weak neutral current couplings) [2]. While two to three sigma effects routinely come and go in physics, it will nevertheless be interesting to watch where the final top mass and electroweak asymmetry averages wind up in the next few years. The SLD result is contributing substantially towards pulling the top mass higher than that predicted by the LEP asymmetry measurements alone. With the SLC now providing 80% polarized electron beam and on the order of 100,000 Z bosons next year, the SLD experiment should be able to reduce the error on $\sin^2\theta_W^{\rm eff}$ (as determined by the A_{LR} measurement) by a factor of two.

5 Acknowledgment

I thank the personnel of the SLAC Accelerator Department and the technical staffs of our collaborating institutions for their outstanding efforts on our behalf. This work was supported in part by Department of Energy contract DE–AC03–76SF00515 (SLAC), the National Science Foundation, the Istituto Nazionale di Fisica Nucleare of Italy, the Japan–U.S. Cooperative Research Project on High Energy Physics, and the Science and Engineering Research Council of the United Kingdom.

References

[1] A. Olchevski, this conference.

[2] A. Blondel *et al.*, "Constraints on Standard Model Parameters from Combined Preliminary Data of the LEP Experiments," LEPEWWG/94–02, July 1994.

[3] C. Campagnari and Qizhong Li-Demarteau, this conference.

[4] F. Abe *et al.*, FERMILAB–PUB–94–097–E, April 1994.

[5] S. Abachi *et al.*, *Phys. Rev. Lett.* **72**, 2138 (1994).

[6] L. Montanet *et al.*, "Review of Particle Properties," *Phys. Rev.* **D50** 1173 (1994).

[7] M. Demarteau *et al.*, "Combining W Mass Measurements," CDF/PHYS 2552 and D0NOTE 2115.

[8] C. Y. Prescott, "Prospects for Polarized Electrons at High Energies," SLAC–PUB–2630, October 1980

[9] D. Calloway *et al.*, SLAC–PUB–6423, April 1994.

[10] Robert Dean Elia, Ph.D. thesis, SLAC Report–429, April 1994.

[11] F.J. Decker, private communication.

[12] Since the colliding electron and positron bunches are produced on different machine cycles and since the electron helicity of each cycle is chosen randomly, any positron helicity arising from the polarization of the production electrons is uncorrelated with electron helicity at the interaction point. The net positron polarization from this process vanishes rigorously. However, positron polarization of constant helicity does affect the measurement.

[13] T. Maruyama *et al.*, *Phys. Rev.* **B46**, 4261 (1992).

[14] K. Abe *et al.*, *Phys. Rev. Lett.* **70**, 2515 (1993).

[15] K. Abe *et al.*, *Phys. Rev. Lett.* **73**, 25 (1994).

[16] L.G. Levchuk, "The intra-atomic motion of bound electrons as a possible source of the systematic error in electron beam polarization measurements by means of a Möller polarimeter," *Nucl. Instrum. Methods* **A345**, 496 (1994).

[17] M. Swartz *et al.*, SLAC–PUB–6467, April 1994.

SLD Collaboration Members and their Institutions

K. Abe,[29] I. Abt,[14] T. Akagi,[27] W.W. Ash,[27] D. Aston,[27] N. Bacchetta,[21] K.G. Baird,[24] C. Baltay,[33] H.R. Band,[32] M.B. Barakat,[33] G. Baranko,[10] O. Bardon,[16] T. Barklow,[27] A.O. Bazarko,[11] R. Ben-David,[33] A.C. Benvenuti,[2] T. Bienz,[27] G.M. Bilei,[22] D. Bisello,[21] G. Blaylock,[7] J.R. Bogart,[27] T. Bolton,[11] G.R. Bower,[27] J.E. Brau,[20] M. Breidenbach,[27] W.M. Bugg,[28] D. Burke,[27] T.H. Burnett,[31] P.N. Burrows,[16] W. Busza,[16] A. Calcaterra,[13] D.O. Caldwell,[6] D. Calloway,[27] B. Camanzi,[12] M. Carpinelli,[23] R. Cassell,[27] R. Castaldi,[23] A. Castro,[21] M. Cavalli-Sforza,[7] E. Church,[31] H.O. Cohn,[28] J.A. Coller,[3] V. Cook,[31] R. Cotton,[4] R.F. Cowan,[16] D.G. Coyne,[7] A. D'Oliveira,[8] C.J.S. Damerell,[25] S. Dasu,[27] R. De Sangro,[13] P. De Simone,[13] R. Dell'Orso,[23] M. Dima,[9] P.Y.C. Du,[28] R. Dubois,[27] B.I. Eisenstein,[14] R. Elia,[27] D. Falciai,[22] C. Fan,[10] M.J. Fero,[16] R. Frey,[20] K. Furuno,[20] T. Gillman,[25] G. Gladding,[14] S. Gonzalez,[16] G.D. Hallewell,[27] E.L. Hart,[28] Y. Hasegawa,[29] S. Hedges,[4] S.S. Hertzbach,[17] M.D. Hildreth,[27] J. Huber,[20] M.E. Huffer,[27] E.W. Hughes,[27] H. Hwang,[20] Y. Iwasaki,[29] P. Jacques,[24] J. Jaros,[27] A.S. Johnson,[3] J.R. Johnson,[32] R.A. Johnson,[8] T. Junk,[27] R. Kajikawa,[19] M. Kalelkar,[24] I. Karliner,[14] H. Kawahara,[27] H.W. Kendall,[16] M.E. King,[27] R. King,[27] R.R. Kofler,[17] N.M. Krishna,[10] R.S. Kroeger,[18] J.F. Labs,[27] M. Langston,[20] A. Lath,[16] J.A. Lauber,[10] D.W.G. Leith,[27] X. Liu,[7] M. Loreti,[21] A. Lu,[6] H.L. Lynch,[27] J. Ma,[31] G. Mancinelli,[22] S. Manly,[33] G. Mantovani,[22] T.W. Markiewicz,[27] T. Maruyama,[27] R. Massetti,[22] H. Masuda,[27] E. Mazzucato,[12] A.K. McKemey,[4] B.T. Meadows,[8] R. Messner,[27] P.M. Mockett,[31] K.C. Moffeit,[27] B. Mours,[27] G. Müller,[27] D. Muller,[27] T. Nagamine,[27] U. Nauenberg,[10] H. Neal,[27] M. Nussbaum,[8] Y. Ohnishi,[19] L.S. Osborne,[16] R.S. Panvini,[30] H. Park,[20] T.J. Pavel,[27] I. Peruzzi,[13] L. Pescara,[21] M. Piccolo,[13] L. Piemontese,[12] E. Pieroni,[23] K.T. Pitts,[20] R.J. Plano,[24] R. Prepost,[32] C.Y. Prescott,[27] G.D. Punkar,[27] J. Quigley,[16] B.N. Ratcliff,[27] T.W. Reeves,[30] P.E. Rensing,[27] L.S. Rochester,[27] J.E. Rothberg,[31] P.C. Rowson,[11] J.J. Russell,[27] O.H. Saxton,[27] T. Schalk,[7] R.H. Schindler,[27] U. Schneekloth,[16] B.A. Schumm,[15] A. Seiden,[7] S. Sen,[33] V.V. Serbo,[32] M.H. Shaevitz,[11] J.T. Shank,[3] G. Shapiro,[15] S.L. Shapiro,[27] D.J. Sherden,[27] C. Simopoulos,[27] N.B. Sinev,[20] S.R. Smith,[27] J.A. Snyder,[33] P. Stamer,[24] H. Steiner,[15] R. Steiner,[1] M.G. Strauss,[17] D. Su,[27] F. Suekane,[29] A. Sugiyama,[19] S. Suzuki,[19] M. Swartz,[27] A. Szumilo,[31] T. Takahashi,[27] F.E. Taylor,[16] E. Torrence,[16] J.D. Turk,[33] T. Usher,[27] J. Va'vra,[27] C. Vannini,[23] E. Vella,[27] J.P. Venuti,[30] P.G. Verdini,[23] S.R. Wagner,[27] A.P. Waite,[27] S.J. Watts,[4] A.W. Weidemann,[28] J.S. Whitaker,[3] S.L. White,[28] F.J. Wickens,[25] D.A. Williams,[7] D.C. Williams,[16] S.H. Williams,[27] S. Willocq,[33] R.J. Wilson,[9] W.J. Wisniewski,[5] M. Woods,[27] G.B. Word,[24] J. Wyss,[21] R.K. Yamamoto,[16] J.M. Yamartino,[16] X. Yang,[20] S.J. Yellin,[6] C.C. Young,[27] H. Yuta,[29] G. Zapalac,[32] R.W. Zdarko,[27] C. Zeitlin,[20] and J. Zhou[20]

[1]Adelphi University, Garden City, New York 11530
[2]INFN Sezione di Bologna, I-40126 Bologna, Italy
[3]Boston University, Boston, Massachusetts 02215
[4]Brunel University, Uxbridge, Middlesex UB8 3PH, United Kingdom
[5]California Institute of Technology, Pasadena, California 91125
[6]University of California at Santa Barbara, Santa Barbara, California 93106
[7]University of California at Santa Cruz, Santa Cruz, California 95064
[8]University of Cincinnati, Cincinnati, Ohio 45221
[9]Colorado State University, Fort Collins, Colorado 80523
[10]University of Colorado, Boulder, Colorado 80309
[11]Columbia University, New York, New York 10027
[12]INFN Sezione di Ferrara and Università di Ferrara, I-44100 Ferrara, Italy
[13]INFN Lab. Nazionali di Frascati, I-00044 Frascati, Italy
[14]University of Illinois, Urbana, Illinois 61801
[15]Lawrence Berkeley Laboratory, University of California, Berkeley, California 94720
[16]Massachusetts Institute of Technology, Cambridge, Massachusetts 02139
[17]University of Massachusetts, Amherst, Massachusetts 01003
[18]University of Mississippi, University, Mississippi 38677
[19]Nagoya University, Chikusa-ku, Nagoya 464 Japan
[20]University of Oregon, Eugene, Oregon 97403
[21]INFN Sezione di Padova and Università di Padova, I-35100 Padova, Italy
[22]INFN Sezione di Perugia and Università di Perugia, I-06100 Perugia, Italy
[23]INFN Sezione di Pisa and Università di Pisa, I-56100 Pisa, Italy
[24]Rutgers University, Piscataway, New Jersey 08855
[25]Rutherford Appleton Laboratory, Chilton, Didcot, Oxon OX11 0QX United Kingdom
[27]Stanford Linear Accelerator Center, Stanford University, Stanford, California 94309
[28]University of Tennessee, Knoxville, Tennessee 37996
[29]Tohoku University, Sendai 980 Japan
[30]Vanderbilt University, Nashville, Tennessee 37235
[31]University of Washington, Seattle, Washington 98195
[32]University of Wisconsin, Madison, Wisconsin 53706
[33]Yale University, New Haven, Connecticut 06511